Chapter 6
Ultra High-Strength Maraging Steel

Abstract Maraging steels are high-strength steels combined with good toughness. They are used particularly in aerospace and tooling applications. Maraging refers to the ageing of martensite, a hard microstructure commonly found in steels. Research on the kinetics of precipitate formation and austenite reversion in maraging steels has received great attention due to their importance to steel properties. Judging from the literature in recent years, research into maraging steels has been very active, mainly extending to new types of steels, for new applications beyond the traditional strength requirements. This chapter provides an in-depth overview of the literature in this area. It includes a state-of-the-art review of ultra high-strength steels, and discussions on types of maraging steels, and microstructure and precipitates in maraging steels.

## 6.1 State-of-the-Art of Ultra High-Strength Steels

Steels combining properties of ultrahigh-strength (UHS) and good ductility are of great importance in automotive, aerospace, nuclear, gear, bearing and other industries. They are the future key materials for lightweight engineering design strategies and corresponding CO_2 savings. Driven by the development of metallurgy and in response to commercial demands, both academia and industry have made great efforts to develop a large variety of steel grades and processing technology, and hence achieved continuous improvement for some decades.

Conventionally produced bulk high-strength steels are known as high-strength low-alloy (HSLA) or microalloyed steels (Chap. 2). This family of steels usually has a strength not exceeding 700–800 MPa and a microstructure of fine-grained ferrite that has been strengthened with carbon and/or nitrogen precipitates of titanium, vanadium or niobium. These steels can be manufactured under relatively well-established processing conditions and have been widely applied for weight reduction in automotive and general construction applications. In order to further enhance the combination of strength and ductility, more alloying elements have been added and more sophisticated alloy systems have been designed employing various mechanisms including dual phase (DP) steels, transformation induced

plasticity (TRIP) steels, twinning induced plasticity (TWIP) steels and maraging steels. Typical strength-ductility profiles of those steel families are shown in Fig. 6.1. Dual phase steels have a microstructure of mainly soft ferrite, with islands of hard martensite dispersed throughout. The strength level of these grades is related to the amount of martensite in the microstructure along with its distribution and morphology. TRIP steels are multiphase grades that involve special alloying and heat treatments to stabilise some amount of austenite at room temperature embedded in a primary ferritic matrix. During plastic deformation and straining, the retained austenite progressively transforms to martensite with increasing strain. This leads to a volume and shape change within the microstructure, which accommodates the strain and increases the ductility. Unlike DP and TRIP steels, TWIP steels generally have a fully austenitic microstructure at room temperature. The formation of mechanical twins during deformation generates high strain hardening, preventing necking and thus maintaining a very high strain capacity and achieving a better combination of strength and ductility. Another important category of UHS steels is maraging steels, in which martensite is formed upon quenching following solution treatment and subsequently further strengthened by the formation of various precipitates such as Cu clusters, Ni_3Ti, NiAl and other types of intermetallics at a moderate temperature of about 500 °C. The superior properties of maraging steels, such as ultra high strength, high ductility, good hardenability, good weldability, simple heat treatment without deformation steps, sometimes in combination with good corrosion resistance, have led to widespread application of maraging steels for demanding applications. The composition and mechanical properties of some successful maraging steel grades are summarised in Table 6.1. All steels in this table except 300 M, Aermet 100 and Low Ni are stainless grades.

In applications of UHS steels, such as in the automotive, aerospace and nuclear industries, the materials are usually subjected to extreme mechanical loads and harsh environmental conditions in which corrosion is an important issue. However, the most commonly used steels for these applications, such as maraging

Fig. 6.1 The strength-ductility profile of various steels. The symbols indicate the properties of existing high-end maraging steel grades
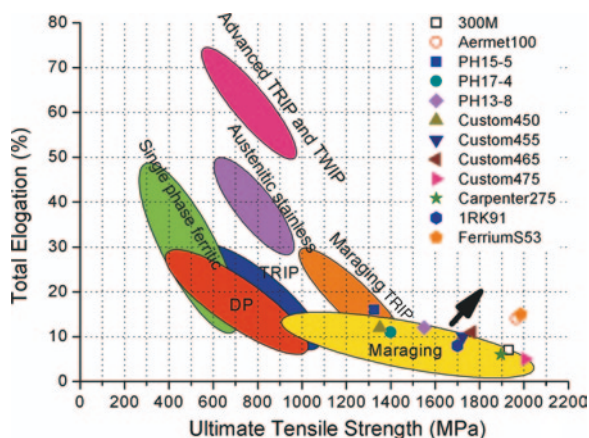
Table 6.1 Compositions in weight per cent, yield strength (YS), ultimate tensile strength (UTS) and elongation (El) of some grades of maraging steels

Steel	C	Cr	Ni	Mo	Cu	Mn	Si	Others	YS (MPa)	UTS (MPa)	El
300 M	0.4	0.8	1.8	0.4	–	0.8	1.6	V (0.05)	1586	1995	0.10
Aermet 100	0.23	3.10	11.1	1.2	–	–	–	Co (13.4)	1724	1965	0.14
PH15-5	<0.07	14–15.5	3.5–5.5	–	2.5–4.5	<1.0	–	–	1228	1325	0.16
PH17-4	<0.07	15.5–17.5	3.0–5.0	–	3.0–5.0	<1.0	<1.0	–	1275	1399	0.11
PH13-8	<0.05	12.3–13.3	7.5–8.5	2.0–2.5	–	<0.1	–	Al (0.90–1.35)	1448	1551	0.12
Custom450	<0.05	14.0–16.0	5.0–7.0	0.5–1.0	1.3–1.8	<1.0	<1.0	–	1296	1351	0.12
Custom455	<0.05	11.0–12.5	7.5–9.5	–	1.5–2.5	<0.5	<0.5	Ti (0.8–1.4), Nb (0.1–0.5)	1689	1724	0.10
Custom465	<0.02	11.0–12.5	10.8–11.3	0.75–1.25	–	<0.25	–	Ti (1.5–1.8)	1707	1765	0.11
Custom475	<0.01	10.5–11.5	7.5–8.5	4.5–5.5	–	<0.5	–	Co (8.0–9.0), Al (1.0–1.5)	1972	2006	0.05
Carpenter275	<0.02	11.0–12.5	10.8–11.3	0.75–1.25	–	<0.25	–	Ti (1.55–1.80), Nb (0.15–0.30)	1758	1896	0.06
1RK91	0.01	12.2	9.0	4.0	1.95	0.32	0.15	Ti (0.87)	1500	1700	0.08
FerriumS53	0.20	10.0	5.5	2.0	–	–	–	Co (14.0), W (1.0), V (0.3)	1517	1986	0.15
Low Ni	0.046	0.20	12.94	1.01	–	<0.01	<0.05	Al (1.61), Nb (0.23)	–	1594	–

300 M for aircraft landing gear, and DP/TRIP in automotive industry, are non-stainless steel grades. Consequently, a specialised and costly coating or plating process has to be employed for corrosion protection. From manufacturing, environmental and reliability considerations, a stainless steel with equivalent mechanical properties but not requiring a corrosion protective coating would be an attractive alternative. Among existing stainless steels, the majority are austenitic, ferritic or duplex (austenite and ferrite) grades. Therefore, much effort for developing ultra high-strength stainless steels have been undertaken, employing martensite as the matrix and strengthening further by various precipitates, while a high Cr content is imposed to ensure corrosion resistance. Some successful grades of these maraging stainless steels are shown in Table 6.1. Notwithstanding the efforts to develop high-strength and high ductility stainless steels, Table 6.1 shows that few stainless steels meet the properties of their non-stainless counterparts in terms of strength and ductility, because of the nature of ferrite and austenite.

6.2 Types of Maraging Steels

Precipitation hardening is one of the most effective mechanisms for increasing the strength of metallic high performance materials. The chemical and crystallographic relations of particles and matrix determine the precipitation behaviour and consequently the material's properties. Precipitation hardening was discovered, a century ago, in aluminium alloys. The principle of particle strengthening is hindering of dislocation movement by the precipitation of nanometre-sized particles. In steels, particle strengthening can either be caused by the precipitation of carbides, e.g. in so-called secondary hardening low-alloy steels, or intermetallic phases, e.g. in so-called maraging steels. Secondary hardening steels are also the major steel grade for today's tool steels. Generally, secondary hardening steels exhibit a complex microstructure depending on alloy composition and the heat treatment applied. The heat treatment consists of hardening, which denotes austenitising in the gamma phase field followed by quenching, and tempering, usually several times. The precipitation of the nanometre-sized carbides has been the focus of numerous studies, and is still a subject of research activities.

The second group of particle-strengthened steels, the maraging steels, was developed over the past 70 years. The term 'maraging' refers to the ageing of martensite, but specifically a martensite that is easily obtained at *low* cooling rates due to a high Ni content in the steel. In addition, these steel grades have very low carbon content and as implied above can belong to the wider group of ultra high-strength steels. Their development started in the 1940s in the USA, when it was noticed that magnetic Fe–Ni–Ti–Al alloys could be hardened significantly by heat treatment. After an initial development period and the addition of Co and Mo, the first applications of maraging steels were set out in the 1960s. Then, the primary goal was to develop high-strength steels for submarine hulls, but maraging steels proved unsuitable for these applications. However, besides a market developed

for specialised aerospace and military applications of these first maraging grades, applications for tools and dies became common. Due to the sharp drop in availability and rising cost of Co in the late 1970s, alternatives to cobalt containing maraging steels were in demand. Thus, much effort was made on developing Co-free maraging steels with appropriate mechanical properties (Sha and Guo 2009). This resulted in a variety of steels with different precipitating elements, e.g. Al, Ti and Cu, and additionally, alloys with lowered Ni contents. One example of these developments is the PH13-8Mo types (Sha and Guo 2009). These cobalt-free alloys generally have inferior properties to the cobalt containing grades, but their properties appear satisfactory for their designed applications, and the absence of cobalt is a distinctive cost advantage.

Intermetallic phases have many specific features as they differ from carbides and thus materials that are strengthened by intermetallic precipitates are of great interest for industrial applications. Specifically, they differ from carbides in the following ways:

(1) Intermetallic phases are formed during primary crystallisation without eutectic transformation, because of which they distribute much more evenly in the cast steel and consequently also in the deformed steel than carbides do. Because of the primary crystallisation we already have a homogeneous distribution in the as-cast state, which is not the case for eutectic solidification. When such a material is deformed the distribution is still homogeneous. In contrast, eutectic carbides, which actually form a network, become more or less homogeneously distributed by deformation (forging or rolling) which is always worse. Intermetallic particle size is also smaller, up to 2–3 μm in diameter. Because of this, intermetallic phases have a less detrimental effect on the strength and ductility and on the variations of these properties depending upon the degree of deformation.

(2) Intermetallic phases precipitate from supersaturated solution during ageing to result in precipitation hardening. The composition of these precipitated phases does not differ from that of the phases mentioned above, i.e. appearing during solidification and present in hot rolling, etc. Precipitation of intermetallic phases is characterised by the following essential features.

(i) The dispersion of intermetallic particles being formed is significant: at the maximum hardness, their size is less than 5–20 nm and the distances between particles around 100 nm, which is lower than the respective values for carbides.

(ii) The distribution of precipitated particles is relatively uniform, since they form in low-carbon or carbon-free martensite (or austenite), especially when Ni is present in the solution. For that reason, the embrittlement effect of the precipitation hardening, even with fine particles, is weaker than that of carbides. However, the embrittling effect of intermetallics does increase with increasing volume fraction.

(iii) The strengthening effect of precipitated intermetallics is very high, greater than with carbides. It is a function of the structure of the matrix,

being greater for a martensitic matrix when compared to an austenitic one. Precipitation hardening increases the hardness by 20–40 HRC for carbon-free martensite (against 3–10 HRC with carbides) and by ~30 HRC for austenite. This is due to the more refined dispersion of intermetallic phases precipitated, with higher volume fractions, compared with carbides.

(3) The temperatures of precipitation hardening which produce the maximum rise in hardness depend on the composition of the metallic matrix and the type of precipitated intermetallic compounds. For martensitic steels, they are lower when intermetallic compounds $(Fe,Ni,Co)_7(Mo,W)_6$ and $(Fe,Cr)_3(Ti,Al)$ precipitate, around 500–550 °C, and higher for the intermetallic phase $(Fe,Co)_7(W,Mo)_6$, around 580–650 °C. In austenitic alloys, these processes are shifted towards still higher temperatures, 750–800 °C and higher. For that reason, steels based on carbon-free martensite can acquire a very high hardness, up to 68–69 HRC, and an increased thermal stability, up to 600–720 °C, depending on the type of intermetallic phase. Austenitic steels have a still higher thermal stability, but a lower hardness.

(4) During precipitation hardening of nickel-containing steels, their hardness rises intensively during the first 10–15 min, but then attains its maximum only after a long holding, 5–10 h, instead of 30–40 min required in carbide strengthening.

(5) Coagulation of precipitated phases and, therefore, reduction in hardness, occur at correspondingly higher temperatures of ageing.

Generally, there are different ways as to how steel grades can be classified, e.g. according to their composition, or strength levels. Such a classification is also possible for maraging steels. A classification according to the main alloy system gives the best overview for maraging steels. The Fe–Ni-Mo system is briefly described in the following.

The first alloys, e.g. Fe-28Ni-4Ti-4Al identified and further work with the Co-Mo hardening system led to the development of the well-known maraging steels based on the Fe–Ni-Mo system, namely the well-known 18Ni (200), 18Ni (250) and 18Ni (300) alloys (Table 6.2). The numbers in parenthesis refer to the nominal yield strengths in ksi (pound-force per square inch, lbf/in^2) in the aged condition. Titanium was also added to this group of alloys as a supplemental hardener. In these alloys, hardening is produced by the combination of Co and Mo as Co

Table 6.2 Nominal compositions (wt%) and the respective yield strength (YS) of commercial maraging steels (Inco)

Alloy designation	Ni	Mo	Co	Ti	Al	YS (MPa)
18Ni (200)	18	3.3	8.5	0.2	0.1	1400
18Ni (250)	18	5.0	8.5	0.4	0.1	1700
18Ni (300)	18	5.0	9.0	0.7	0.1	2000
18Ni (350)	18	4.2	12.5	1.6	0.1	2400
18Ni (cast)	17	4.6	10.0	0.3	0.1	1650

lowers the solubility of Mo and thus increases the amount of Mo-rich precipitates that form during ageing. A number of studies have been conducted on the precipitation behaviour of these maraging steels. Overall, the following precipitation reactions take place during ageing. Strengthening in the underaged conditions is caused by Mo-rich zones. With further ageing, the metastable orthorhombic Ni_3Mo forms which transforms into $Fe_2(Mo,Ti)$ hexagonal Laves phase after longer ageing. The formation of Ni_3Mo is accelerated by Co. However, it is suggested that higher Ti contents (alloy 350) lead to the formation of Ni_3Ti instead of Ni_3Mo.

As mentioned above, around 1978–80, development of cobalt-free grades was promoted (Sha and Guo 2009). Considering that the goal was the development of high fracture toughness in cobalt-free maraging steel, various elements that might successfully substitute for Co were considered. An analysis of a number of variants revealed that the alloy should contain 3 % Mo and 1.4 % Ti to achieve the desired yield strength of 250 ksi (1700 MPa) with good transverse ductility. Ni_3Ti was found to be the major precipitation-hardening phase in cobalt-free maraging steels, whereas the achieved yield strength rises with increased Mo and Ti contents (up to 2400 MPa). The mechanism of strengthening and toughening is the same in low and high Mo and Ti containing alloys. However, the high Mo and Ti alloys additionally contain a large number of coarse particles of type Fe_2Ti and $Fe_2(Mo,Ti)$ embedded in the martensite lath boundary or within the lath. Those particles produce a detrimental effect on fracture toughness and ductility.

Other maraging systems include broadly Fe–Ni-Cr and Fe–Ni-Mn, which will be discussed in the following sections.

6.3 Microstructure and Precipitates in Maraging Steels

6.3.1 PH13-8Mo Maraging Steels

The microstructural constituents that were observed in PH13-8Mo maraging steels include the following:

(1) δ ferrite
(2) cubic martensite
(3) retained and reverted austenite
(4) nanometre-sized precipitates of intermetallic type
(5) Laves phase.

A phase that is sometimes present in PH13-8Mo maraging steels is δ ferrite, the high temperature bcc ferrite. The presence of this phase is associated with the alloy composition and production route. Although the solidification path of the PH13-8Mo steel grades is known to be fully ferritic via the δ phase, the transformation of δ → γ strongly depends on cooling rate. Thus, large cast sizes and an appropriate composition can provoke the incomplete transformation of δ → γ.

PH13-8Mo maraging steels receive their excellent combination of strength and ductility by a heat treatment which consists of a first-step solution anneal in the temperature range 900–1000 °C and subsequent air-cooling to room temperature. When quenched from the austenitic single-phase field after solution annealing, the austenite transforms into a soft, but heavily dislocated Ni-martensite, exhibiting a cubic structure. The martensite in this steel grade is of lath type and it forms a packet that consists of many similar-sized laths arranged parallel to each other. Each prior austenite grain includes several lath packets.

Depending mainly upon the Ni content, but also on all other alloying elements, a certain amount of austenite can be retained after quenching to room temperature. Besides this retained austenite, which is the result of a martensite finish temperature below room temperature, a so-called 'reverted austenite' can also be present in maraging steels. The occurrence of this reverted austenite also depends upon chemical composition, but additionally, the applied ageing temperature and time play decisive roles. The reverted austenite emerges from martensite during ageing at temperatures below the global $\alpha \rightarrow \gamma$ transformation temperature. This is the temperature where the entire material transforms, which is significantly higher than the local temperature because of Ni-enrichment.

Ageing, typically carried out in a temperature range of 400–600 °C, leads to the precipitation of the strengthening nanometre-sized intermetallic particles.

Laves phases formed at higher ageing temperatures have also been observed in this steel grade.

However, the nanometre-sized precipitates and the austenite phase fraction have the strongest effect on the mechanical properties of maraging steels and, thus, a more detailed survey of the literature for these aspects is given in the following.

6.3.2 Precipitates

The precipitation behaviour and strengthening mechanisms in cobalt-free maraging steels have been extensively studied by employing a variety of characterisation techniques. It has been shown that maraging steels containing Ni and Al are strengthened by the formation of the ordered β'-NiAl phase with B2 (CsCl) superlattice structure (Sha and Guo 2009). This structure consists of two interpenetrating primitive cubic cells, where the Al atoms occupy the cube corners of the first sublattice and the Ni atoms occupy the cube corners of the second sublattice. The lattice constant of the stoichiometric composition is 0.2887 nm. This is very close to the lattice constant for ferrite, which has a value of 0.28664 nm. Due to this fact, the NiAl precipitates are coherent with the matrix and even remain coherent after long ageing times. Precipitation takes place immediately after heating the material to the ageing temperature. Sha and Guo (2009) show Ni- and Al-rich clusters after just 6 min of ageing at 593 °C and after 40 min of ageing at 510 °C. However, the composition of the precipitates, even after longer ageing times, is far from stoichiometric NiAl phase, the precipitates containing a significant amount of Fe. The shape of

the precipitates is a matter of debate in the literature. In general, the NiAl phase is believed to be of spherical shape, but some authors assume a change of morphology from spherical- to needle- and plate-shaped forms at longer ageing times. However, it is generally thought that their formation proceeds via solute-rich clusters within the martensitic matrix. Out of these nuclei, the coherent NiAl precipitates are formed and distributed uniformly within the matrix (Leitner et al. 2010).

In contrast, it has been reported that strengthening in Ti-containing maraging steels is caused by the precipitation of the η-phase ($Ni_3(Ti,Al)$) (Leitner et al. 2010). The η-phase exhibits a hexagonal lattice with $a = 0.255$ nm and $c = 0.42$ nm. In the literature, some debate exists on the mechanism of formation of the η-phase. In most studies, heterogeneous nucleation on dislocations is proposed, with subsequent growth taking place via pipe diffusion (Dutta et al. 2001). Others advance the theory that formation of coherent zones on dislocations in the martensitic matrix takes place first, acting as nucleation sites for the η precipitates (Leitner et al. 2010). There is also some discrepancy on the dominating strengthening mechanism in this kind of maraging steels. While the majority of studies attributed strengthening to the formation of Ni_3Ti, others proposed an additional contribution from some B2-type ordering of Fe and Ni atoms in the matrix (Leitner et al. 2010).

A further type of precipitate phase, called G-phase, was found in Ti-containing maraging steels alloyed with Si. The G-phase exhibits the chemical composition $Ti_6Si_7Ni_{16}$ and precipitates primarily on grain boundaries. Depending upon the chemical composition of the alloy, the G-phase ($Ti_6Si_7Ni_{16}$) and the η-phase (Ni_3Ti) can precipitate either simultaneously or separately. The shape of the Ni_3Ti-phase was thought to be rod-like, whereas the G-phase shows a spherical morphology. Later studies revealed that both the spherical G-phase and the rod-shaped η-phase are formed independently out of an undefined precursor phase, which is responsible for strengthening up to peak hardness. Atom probe tomography (APT) was used to follow the precipitation sequence in an Si-free Fe–Cr–Ni–Al–Ti stainless steel during ageing at 525 °C (Schober et al. 2009). In that work, instead of splitting into G-phase ($Ti_6Si_7Ni_{16}$) and η-phase (Ni_3Ti), the formation of spherical NiAl particles and elongated $Ni_3(Ti,Al)$ particles out of an undefined precursor phase in the early stages was found.

A further age-hardener in maraging steels is copper. It is used in PH15–5 and PH17–4 alloys as a precipitating hardening element, but also in alloy systems such as 1RK91 (Sandvik in-house grade designation) and C455 (Custom455, a registered trademark of Carpenter Technology Corporation) (for compositions see Table 6.1) as nucleation site for the precipitation of the strengthening causing phase (Schnitzer et al. 2010a).

In the case of 1RK91, the precipitation sequence starts with the formation of an Ni, Ti and Al-rich phase nucleating on Cu-rich clusters (Schnitzer et al. 2010a). During further ageing, $Ni_3(Ti,Al)$ precipitates develop adjacent to Cu-rich precipitates. The C455, which contains less Al and no Mo, forms clusters of Cu, Ti and Ni at the early stages, and they are thought to be a precursor phase of η-Ni_3Ti (Schnitzer et al. 2010a). An extended ageing treatment then leads to the separation of Ni-rich (η-Ni_3Ti) and Cu-rich precipitates. The effect of Cu on the precipitation

evolution in PH13-8Mo type maraging steel, which exhibits NiAl and η-phase pre-
cipitates, was recently investigated by Schnitzer et al. (2010a). This study revealed
the formation of NiAl out of a Cu-containing precursor phase and the nucleation
of η-phase on independent Cu clusters.

There exists almost a comprehensive picture of precipitation behaviour in
PH13-8Mo type maraging steels. Only the influence of Cu on the formation of
G-phase is missing.

Additionally to the strengthening precipitates, the formation of carbides has
been observed in maraging, although the carbon content is generally very low
in such steels. These carbides precipitate adjacent to or inside reverted austenite
because of the higher carbon solubility in austenite. The carbides were found to be
of type $Cr_{23}C_6$ and $(Cr,Mo)_2C$.

6.4 Reverted Austenite and Mechanical Properties

6.4.1 Reverted Austenite

In maraging steels, partial reversion from martensite to austenite can take place
during ageing below the global $\alpha \rightarrow \gamma$ temperature (Schober et al. 2009). The
amount of reverted austenite present after ageing depends on the ageing tem-
perature as well as ageing time (Sha and Guo 2009). The formation of reverted
austenite is reported to be the result of local Ni-enrichment, which arises during
ageing. As Ni, one of the major alloying elements in maraging steels, is an austen-
ite stabilising element, the local transition temperature of martensite to austenite is
lowered. In this area, the applied ageing temperature is, therefore, higher than the
transition temperature from martensite to austenite. Due to this Ni enrichment, this
austenite remains stable even when the material is cooled back to room tempera-
ture. This type of austenite has to be distinguished from retained austenite, which
can also be present in maraging steels after cooling from the solution annealing
temperature. Depending on the alloy composition and the applied heat treatment,
different morphologies of reverted austenite have been observed in maraging
steels, shown in Fig. 6.2. The reverted austenite morphologies are classified into
three types: (i) matrix austenite, (ii) lath-like austenite and (iii) recrystallised aus-
tenite. Matrix austenite (Fig. 6.2a) grows either from retained austenite with the
same orientation, or nucleates on prior austenite grain boundaries and then forms a
single grain. Lath-like austenite (Fig. 6.2b) can develop within the martensite lath
or grow along the lath boundaries of martensite. The growing direction of the aus-
tenite laths is parallel to the martensite lath resulting in a lamellar structure of aus-
tenite and martensite. The elongated shape is supposed to be caused by a growth
impediment of the adjacent martensite laths. Recrystallised austenite (Fig. 6.2c)
forms at higher ageing temperatures or longer ageing times, and is character-
ised by a very low density of defects and dislocations (Viswanathan et al. 2005).
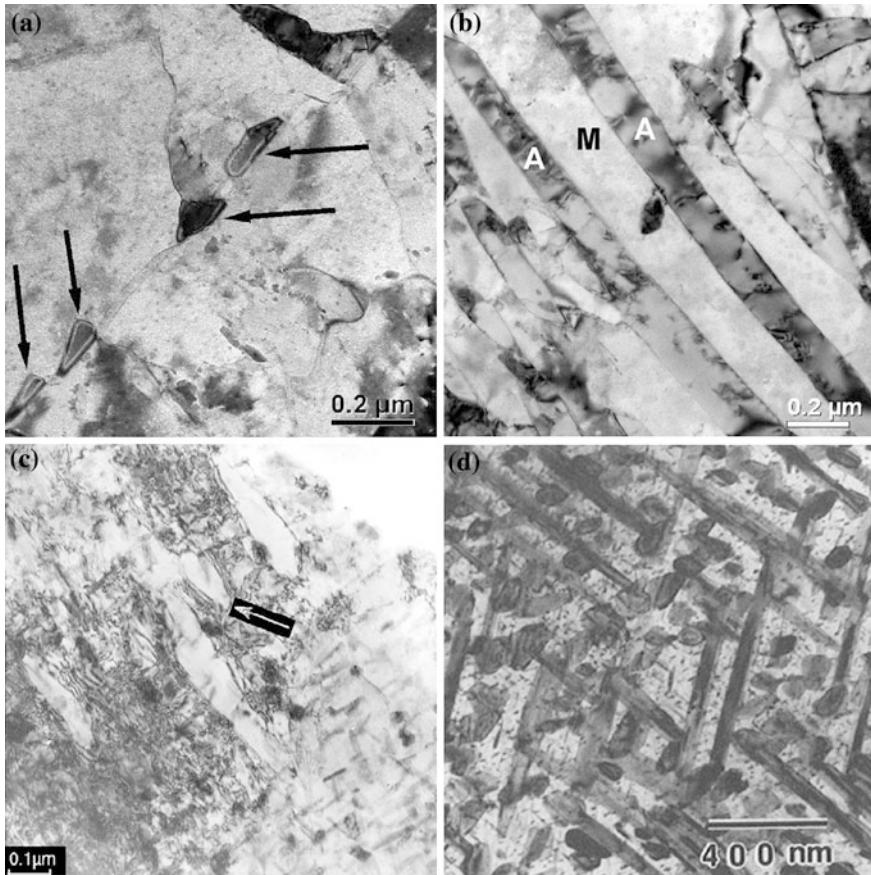
Fig. 6.2 Morphologies of reverted austenite in maraging steels **a** matrix austenite (Schnitzer et al. 2010b), **b** lath-like austenite (A = austenite, M = martensite) (Schnitzer et al. 2010b), **c** recrystallised austenite (Viswanathan et al. 2005), **d** Widmanstätten austenite (Kim and Wayman 1990)

In addition, a fourth morphology found in maraging steels, is Widmanstätten (Fig. 6.2d), only evidenced in high Ni-alloyed and Ti-containing maraging steels (Schnitzer et al. 2010b). The morphology of reverted austenite developed depends on the applied heating rate and on the ageing temperature (Schnitzer et al. 2010c).

Independently of morphology, the orientation relationship between austenite and martensite was found to be either of type Kurdujumov–Sachs, with $(110)_{bcc}//(111)_{fcc}$ and $[111]_{bcc}//[110]_{fcc}$, or Nishiyama-Wassermann with $(110)_{bcc}//(111)_{fcc}$ and $[100]_{bcc}//[110]_{fcc}$ (Schnitzer et al. 2010b).

An important finding for the understanding of the formation of reverted austenite is the fact that the regions of reverted austenite are free of the precipitates causing strengthening. Only carbides precipitate inside the austenite or adjacent to it, due to the higher solubility for carbon in austenite compared to martensite.

The formation mechanism of reverted austenite in maraging steels is supposed to be a diffusion-controlled process. It is assumed that the formation of reverted austenite is connected to the dissolution of precipitates, resulting in a local enrichment of austenite stabilising elements (Sha and Guo 2009). This was also reported for 18 % Ni steels, where the formation of reverted austenite was encouraged by the dissolution of $Ni_3(Mo,Ti)$ precipitates. The formation of reverted austenite can be accompanied by the precipitation of Fe_2Mo. This leads to the assumption that the Ni of the dissolved $Ni_3(Mo,Ti)$ precipitates contributes to the formation of reverted austenite, while the released Mo is used to form Fe_2Mo precipitates. Others exclude the theory that the formation of reverted austenite is related to the dissolution of precipitates. For example, Ni diffuses to dislocations and other defects, resulting in microsegregation of the austenite stabilising elements in localised areas. Hsiao et al. (2002) reported that in Cu-containing maraging alloys, such as PH17-4, fine Cu precipitates act as nucleation sites for austenite formation since both copper and austenite exhibit the same crystallographic structure with similar lattice parameter. Kim and Wayman (1990) suggested that the formation of lath like austenite in high Ni-containing maraging alloys is shear dominated, but assisted by a diffusion-controlled process. Schnitzer et al. (2010b) investigated the formation of reverted austenite in PH13-8Mo type maraging steel. The interpretation of the experimental data was supported by thermodynamic and kinetic calculations. It was shown that the formation of NiAl precipitates and reverted austenite starts from the very beginning of ageing widely independent of each other, i.e. the formation of both, austenite and NiAl nuclei, is thermodynamically possible in the virgin martensitic matrix. Thus, dissolution of precipitates is not necessarily the initial driving factor for the formation of reverted austenite. Consequently, a formation mechanism was proposed as follows: beginning from lath martensite with high dislocation density after solution annealing, NiAl precipitates and reverted austenite nucleate independently. The NiAl precipitates are homogeneously distributed in the martensitic matrix and reverted austenite forms preferentially on prior austenite grain boundaries or on martensite lath boundaries. Growth of reverted austenite is related to dissolution of adjacent NiAl precipitates, whereas the reverted austenite incorporates Ni stemming from the dissolved precipitates. In contrast, the released Al content is transferred to the NiAl precipitates left in the matrix.

6.4.2 Mechanical Properties

Maraging steels belong to the group of high-strength steels, i.e. tensile strength >1000 MPa. The achieved strength values range from 1000 MPa up to 3000 MPa. The stress–strain behaviour is characterised by a yield strength that is above 80 % of the ultimate tensile strength, i.e. the work hardening is small. The reason for this behaviour is proposed to be as follows. The coherent precipitates introduce a friction stress acting on dislocations, which raises the level of the stress–strain curve without markedly altering the dislocation interactions leading to work hardening.

The following microstructural features have an influence on the mechanical properties, in different ways/extents:

(1) Nanometre-sized precipitates
(2) Retained or reverted austenite
(3) Prior austenite grain size.

The required strength and toughness is reached after an ageing treatment, which conforms to the application (Sha and Guo 2009). Of course, the chemical composition, but also the applied ageing temperature and time influence types, size and volume fraction of precipitates as well as the amount of austenite and thus the mechanical properties. In maraging alloys, the main strengthening contribution stems from the precipitation of nanometre-scale precipitates. The high-strength of maraging steels, thereby, is because of dense and homogenously distributed precipitates in the martensitic matrix. Depending upon their size and coherency, they are either sheared or circumvented by dislocations.

Retained and reverted austenite also shows a strong influence on the mechanical properties of maraging steels. Reverted austenite is free of precipitates and possesses a much lower yield strength compared to the martensitic matrix (Sha and Guo 2009). Reverted austenite influences the mechanical properties. Viswanathan et al. (2005) observed a pronounced decrease of the yield strength with increasing amount of reverted austenite. Reverted austenite is supposed to increase the ductility and impact toughness. Therefore, for high toughness requirements, increased amounts of reverted austenite are beneficial and the material is subjected to higher ageing temperatures. On prolonged ageing, coarsening of precipitates results also in an increase of ductility but loss of strength. However, it was reported that the influence of austenite reversion is much more pronounced on softening than the influence of precipitate coarsening (Schnitzer et al. 2010b). In the literature, there are also investigations that report a detrimental effect of reverted austenite. Viswanathan et al. (2005) showed that the ductility is only increased in the early stages of ageing. Severe embrittlement was noticed in samples subjected to prolonged ageing. Reverted austenite in a Co-containing maraging steel leads to deterioration in ductility at low temperatures as fracture occurs along the boundaries of the martensite packets. However, it is known that the austenite phase in maraging steels is not stable during deformation (Schnitzer et al. 2010c), which results in transformation to martensite (so-called transformation induced plasticity, TRIP effect). This transformation behaviour also strongly influences the mechanical properties of maraging steels.

Normally, the amount of austenite is associated with the size of precipitates. Schnitzer et al. (2010c) performed a study on PH13-8 Mo-type maraging steel to judge the individual influence of precipitates and reverted austenite on mechanical properties. Calculation revealed that approximately 40 % of the loss in yield strength during ageing could be attributed to the influence of higher amounts of reverted austenite. The remaining amount of the observed decrease in strength is due to coarsening of NiAl precipitates.

A further microstructure constituent in maraging steels, which may affect the mechanical properties, is the martensitic matrix and thus, the prior austenite grain

size. The grain size depends on the solution treatment temperature as well as time, whereas the martensite lath spacing in maraging steels is independent of the solution treatment temperature (Schnitzer et al. 2010c). The influence of the grain size on mechanical properties depends on the nucleation site of the precipitates. When precipitates nucleate homogenously in the martensitic matrix, no influence of grain size was observed (Schnitzer et al. 2009). In contrast, the relationship between yield strength and grain size follows the Hall–Petch equation after ageing when the precipitates nucleate on grain boundaries.

6.5 Evolution of Precipitates and the Overall Process

A research monograph on maraging steels (Sha and Guo 2009) has described recent theoretical research on the two main types of phase transformation in maraging steels, *precipitation* and *austenite reversion*. Before either of these transformations happens in these steels (during heating), there is a third transformation, which is the martensitic transformation (during cooling). Precipitation and austenite reversion occur in this martensite matrix, the former generally desirable as long as it is not too complete and the latter usually undesirable. In simple terms, precipitation leads to hardening and austenite reversion leads to softening. Although martensitic transformation is a prerequisite of the functioning of maraging steels, it is easily achievable and its details do not strongly determine the final steel properties, at least to a far lesser extent than precipitation and austenite reversion. For this reason, these sections will not consider the martensitic transformation in maraging steel.

Section 6.5.1 will give a brief discussion of the evolution of precipitates in maraging steels, with particular reference to its complexity in inter-particle spacing. This will be followed by the brief Sect. 6.5.2 on the overall transformation process.

6.5.1 Calculation of Inter-Particle Spacing

When precipitation fraction increases, the particle size should not be ignored when calculating the inter-particle spacing L. Assuming that the precipitates are spherical, the relationship between precipitate fraction f, inter-particle spacing and particle radius r is given by Sha and Guo (2009), which also contains the other equation in this section:

$$L = \left(1.23\sqrt{2\pi/(3f)} - 2\sqrt{2/3}\right) r \qquad (6.1)$$

When precipitation fraction increases, the L/r ratio decreases dramatically (Fig. 6.3). L and r become very much comparable when f increases to about 0.1. The simple formula significantly overestimates the inter-particle spacing when the precipitation fraction is large. In addition to Eq. 6.1 for spherical precipitates,

Fig. 6.3 Comparison
of L/r ratio as a function
of precipitation fraction,
bwteeen Eq. 6.1 (solid line)
and the simple formula
$L/r = \sqrt{2\pi/3f}$ (dotted line)
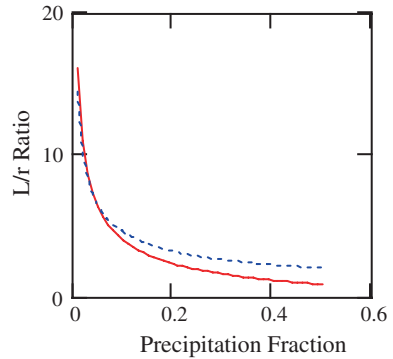
there are equations for plate-like particles, which is the case for Ni_3Ti-type precipi-
tates in maraging steels. If the volume fraction can be estimated using the Johnson–
Mehl–Avrami (JMA) equation, then particle spacing as a function of time will be
known. Such a procedure allows the quantification of age hardening to be carried out
accurately.

The size increment of particles during the early ageing period may follow a
slower procedure than the classical parabolic growth law would allow, regardless
of whether the phase separation follows classical nucleation or spinodal decom-
position. Although sometimes it is difficult to determine the controlling step, and
in turn the operating coarsening law, Lifshitz-Slyozov-Wagner (LSW) theory
(Lifshitz and Slyozov 1961; Wagner 1961) may be used for practical purposes.
The LSW theory is the first statistical mechanical formulation of the kinetics of
precipitate ageing, for diffusion-limited as well as interface-limited precipitate
coarsening. The prediction of LSW theory that the cube of the average length scale
of particles increases linearly with time was validated by numerous experiments,
even in cases where there was a finite volume fraction of the dispersed phase. In
LSW theory, the coarsening rate of a precipitate particle is given by the linear form

$$\frac{dr}{dt} = \frac{K_{LSW}}{r}\left(\frac{1}{r^*} - \frac{1}{r}\right) \tag{6.2}$$

where r and r^* are the radius of the particle, and the critical radius of the precipi-
tate population, respectively. K_{LSW} is the kinetic coefficient and is independent of
the volume fraction of the precipitates.

6.5.2 The Overall Process

The overall transformation curve can be recorded using dilatometry (Fig. 6.4)
measured for a cobalt-free maraging steel as an example. The steel composition
is Fe-18.9Ni-4.1Mo-1.9Ti (wt %). Uniform expansion continues until 510 °C
when a small contraction starts to occur, indicating the start of precipitation at this

Fig. 6.4 Dilatometry curve
of the 2000 MPa grade
cobalt-free maraging steel
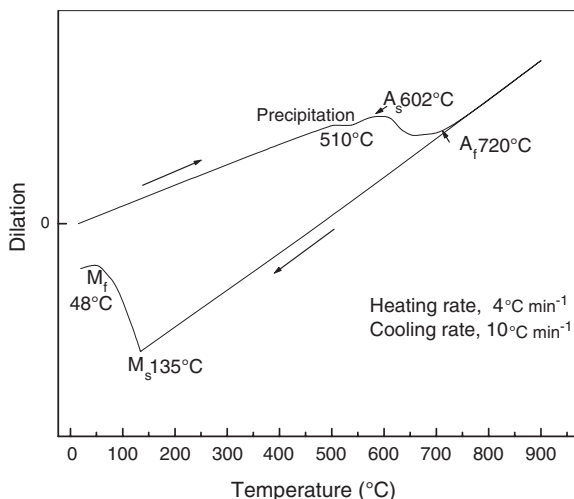
temperature. This is followed by a small period of linear expansion with increasing temperature. When the temperature is raised to 602 °C, a large contraction appears in the dilatometry curve, which can be taken as the start of austenite formation (A_s). At 660 °C, this contraction starts to slow down, until 720 °C when the curve resumes linear expansion. Therefore, the austenite transformation ends at around 720 °C (A_f). Complete solution is ensured by heating continuously to 900 °C and holding at this temperature for 30 min. During cooling to room temperature, there is drastic expansion at approximately 135 °C, due to the sudden start of rapid transformation from austenite to martensite, corresponding to the martensite start temperature, M_s. Martensite finish temperature (M_f) is about 48 °C. Thus, the cobalt-free maraging steel should have a single-phase structure upon cooling to room temperature that is martensite.

A discrepancy in dilatation at room temperature is apparent in Fig. 6.4. In dilatometry curves for T300 (Fe-18Ni-2.4Mo-2.2Ti, wt%) and C350 (Fe-18.77Ni-10.8Co-4.2Mo-1Ti, wt%) recorded in the literature (He et al. 2003), the cooling curve normally does not return to zero but to below the original point. This residual strain may be induced by the martensite phase transformation, due to both thermal and transformation changes. The strength level (2400 MPa) of the commercial cobalt-free T300 steel is the same as the experimental cobalt-free maraging steel used in Fig. 6.4, although the experimental steel, due to its very low impurity levels, has better toughness. The C350 steel is also ultra-purified steel, reaching a strength level of 2800 MPa. The transformation-induced plasticity in the free dilatometry cycle is seen in the martensitic transformation in many experiments (He et al. 2003; Coret et al. 2004). However, the exact mechanism is not clear. It is possible that the lattice has been sheared and it could not return to the original position.

Cobalt raises the martensitic phase transformation temperature. In general, the martensitic transformation temperature in 18Ni maraging steels is 50–100 °C

higher than in their cobalt-free counterparts. However, controlling correctly the amount of nickel and molybdenum in cobalt-free maraging steels can still ensure complete martensitic transformation upon cooling to room temperature after solution treatment.

6.6   Research Trends

Although research in maraging steels usually involves the quantification of phase transformation kinetics, this section will expand beyond this theme, to the general developments in this type of steel. These can be roughly divided into the following areas.

6.6.1   Ultrafine-Grained Fe–Ni–Mn Steels, Novel Maraging Steels and Atom Probe Tomography

The research includes the study of behaviour during isothermal ageing (Nedjad et al. 2009a), the effects of chromium addition (Meimandi et al. 2008) and further alloying (Nedjad et al. 2008a, 2009b) on microstructure and mechanical properties including tensile behaviour (Nedjad et al. 2009c), and the correlation between intergranular brittleness and precipitation reactions (Nedjad et al. 2008b). Transmission electron microscopy studies have been carried out on grain boundary precipitation (Nedjad et al. 2006, 2008c). X-ray diffraction including peak profile analysis (Garabagh et al. 2008a) and microstructural study (Mobarake et al. 2008) have been carried out on a nanostructured 18Ni maraging steel prepared by equal-channel angular pressing (Garabagh et al. 2008b), aimed at better understanding of the deformation process and deformed structure. This equal-channel angular pressing is a natural extension after studying the extent and mechanism of nanostructure formation during cold rolling and ageing of lath martensite (Nedjad et al. 2008d).

Characterisation using advanced equipment and techniques has been carried out, the most recent example being of the precipitation behaviour of intermetallic NiAl particles in Fe-6at.%Al-4at.%Ni by small angle neutron scattering (SANS) and three-dimensional atom probe (3DAP) (Schober et al. 2010). Transformation during continuous-to-isothermal ageing applied on a maraging steel has been studied (Primig and Leitner 2010), as has the effect of Cu on the evolution of precipitation in a Fe–Cr–Ni–Al–Ti maraging steel (Schnitzer et al. 2010a) and the splitting phenomenon (Leitner et al. 2010). In addition, reverted austenite in a PH13-8Mo maraging steel has been investigated (Schnitzer et al. 2010b), in particular its influence on static and dynamic mechanical properties (Schnitzer et al. 2010c). Modelling work has also been carried out on the yield strength of stainless maraging steel (Schnitzer et al. 2010d). The latest techniques of atom probe tomography have been used in this field (Pereloma et al. 2004, 2009; Shekhter et al. 2004).

6.6.2 Computer-Aided Alloy Design Approach
to New Steel Compositions

The design is always followed by characterisation of the steels manufactured on a laboratory scale. Studies include real-time martensitic transformation kinetics in maraging steel under high magnetic fields (San Martin et al. 2010). A novel ultra high-strength stainless steel, strengthened by various coexisting and multi-species (Xu et al. 2008) nanoprecipitates including Ni_3Ti intermetallic, has been designed (Xu et al. 2010a) based on a genetic algorithm and thermokinetics, and has been characterised (Xu et al. 2010b). This genetic computational design of novel ultra high-strength maraging precipitation hardenable stainless steels has incorporated alloy composition as well as austenitisation and ageing temperatures as combined optimisation parameters (Xu et al. 2009a, 2009b); the model description and first experimental validation have been given (Xu et al. 2009c).

Traditionally, new alloys have been developed through an empirical 'trial-and-error' approach, which is based on systematic experimental investigations. This semi-empirical approach is very dependent on intuition, experience and, to some extent, luck. Depending on the matrix type and the strengthening system, modern high-end UHS steels possess intentionally, and with specified amounts, a range of elements such as C, Cr, Ni, Al, Ti, Mo, V, Mn, Nb, Co, Cu, W, Si, B and N in wide ranges of concentrations. The interactions of alloying elements display complex cross effects. To understand the competition, conflict and synergy among various alloying elements experimentally, it would be necessary to systematically produce a large number of alloys with different compositions. Apart from the alloy composition, the heat treatment plays a paramount role in determining mechanical properties as well. After producing trial alloys, processing parameters need to be optimised via a tremendous amount of experimental work to achieve the best mechanical properties. Therefore, the conventional trial-and-error approach has been recognised to have low success rate, and be very costly and time-consuming.

With the improved understanding of processing/structure/property/performance relationships, and with the advent of more powerful and reliable computer hard- and software, alloy design philosophies are now increasingly oriented in the goal/means direction as demonstrated by the chain design model by Olson (1997). The goal/means oriented alloy design approach starts with defining the target properties required by the applications. This first link, between performance and properties, is mainly based on mechanical engineering. In the second step, the target microstructures are subsequently designed to obtain the desired properties, according to metallurgical and mechanical principles. The last link, attaining the tailored microstructures, is the key and most sophisticated process in the goal/means alloy design strategy. The alloy composition and heat treatment parameters are designed and optimised, employing various approaches, to obtain the desired microstructures.

Following fully or partially the goal/means oriented alloy design methodology, computational methods of different types have become a more efficient and powerful

tool in providing guidance for designing new alloys as well as for process development. Thermodynamics aided design approaches have been applied, in different degrees, to various systems such as maraging. Another popular computational approach is artificial neural networks (ANN) which extracts empirical trends from exploring large databases. The neural networks are often coupled with genetic algorithms (GA) for alloy design to fulfil the multi-objective optimisation goals. More recently, atomic level ab initio calculations are also applied to provide theoretical guidance in selecting and optimising composition of Ti-based alloys, stainless steels and UHS steels. With respect to the process development, the experimental approach can also be better guided by extracting information from computational thermodynamics and artificial neural networks.

References

Coret M, Calloch S, Combescure A (2004) Experimental study of the phase transformation plasticity of 16MND5 low carbon steel induced by proportional and non-proportional biaxial loading paths. Eur J Mech A-Solid 23:823–842. doi:10.1016/j.euromechsol.2004.04.006

Dutta B, Palmiere EJ, Sellars CM (2001) Modelling the kinetics of strain induced precipitation in Nb microalloyed steels. Acta Mater 49:785–794. doi:10.1016/S1359-6454(00)00389-X

Garabagh MRM, Nedjad SH, Shirazi H, Mobarekeh MI, Ahmadabadi MN (2008a) X-ray diffraction peak profile analysis aiming at better understanding of the deformation process and deformed structure of a martensitic steel. Thin Solid Films 516:8117–8124. doi:10.1016/j.tsf.2008.04.019

Garabagh MRM, Nedjad SH, Ahmadabadi MN (2008b) X-ray diffraction study on a nanostructured 18Ni maraging steel prepared by equal-channel angular pressing. J Mater Sci 43:6840–6847. doi:10.1007/s10853-008-2992-4

He Y, Liu K, Yang K (2003) Effect of solution temperature on fracture toughness and microstructure of ultra-purified 18Ni(350) maraging steel. Acta Metall Sin 39:381–386

Hsiao CN, Chiou CS, Yang JR (2002) Aging reactions in a 17–4 PH stainless steel. Mater Chem Phys 74:134–142. doi:10.1016/S0254-0584(01)00460-6

Kim SJ, Wayman CM (1990) Precipitation behavior and microstructural changes in maraging Fe-Ni-Mn-Ti alloys. Mater Sci Eng A 128:217–230. doi:10.1016/0921-5093(90)90230-Z

Leitner H, Schober M, Schnitzer R (2010) Splitting phenomenon in the precipitation evolution in an Fe-Ni-Al-Ti-Cr stainless steel. Acta Mater 58:1261–1269. doi:10.1016/j.actamat.2009.10.030

Lifshitz IM, Slyozov VV (1961) The kinetics of precipitation from supersaturated solid solutions. J Phys Chem Solids 19:35–50. doi:10.1016/0022-3697(61)90054-3

Meimandi SH, Nedjad SH, Yazdani S, Ahmadabadi MN (2008) Effect of chromium addition on the microstructure and mechanical properties of Fe-10Ni-6Cr-2Mn maraging steels. In: New developments on metallurgy and applications of high strength steels, TMS, Warrendale, pp 1151–1157

Mobarake MI, Nili-Ahmadabadi M, Poorganji B, Fatehi A, Shirazi H, Furuhara T, Parsa H, Nedjad SH (2008) Microstructural study of an age hardenable martensitic steel deformed by equal channel angular pressing. Mater Sci Eng A 491:172–176. doi:10.1016/j.msea.2008.02.034

Nedjad SH, Ahmadabadi MN, Mahmudi R, Furuhara T, Maki T (2006) Analytical transmission electron microscopy study of grain boundary precipitates in an Fe-Ni-Mn maraging alloy. Mater Sci Eng A 438:288–291. doi:10.1016/j.msea.2006.02.097

Nedjad SH, Garabagh MRM, Ahmadabadi MN, Shirazi H (2008a) Effect of further alloying on the microstructure and mechanical properties of an Fe-10Ni-5Mn maraging steel. Mater Sci Eng A 473:249–253. doi:10.1016/j.msea.2007.05.093

Nedjad SH, Ahmadabadi MN, Furuhara T (2008b) Correlation between the intergranular brit-
tleness and precipitation reactions during isothermal aging of an Fe-Ni-Mn maraging steel.
Mater Sci Eng A 490:105–112. doi:10.1016/j.msea.2008.01.070

Nedjad SH, Ahmadabadi MN, Furuhara T (2008c) Transmission electron microscopy study
on the grain boundary precipitation of an Fe-Ni-Mn maraging steel. Metall Mater Trans A
39A:19–27. doi:10.1007/s11661-007-9407-z

Nedjad SH, Ahmadabadi MN, Furuhara T (2008d) The extent and mechanism of nanostructure
formation during cold rolling and aging of lath martensite in alloy steel. Mater Sci Eng A
485:544–549. doi:10.1016/j.msea.2007.08.008

Nedjad SH, Ahmadabadi MN, Furuhara T (2009a) Annealing behavior of an ultrafine-
grained Fe-Ni-Mn steel during isothermal aging. Mater Sci Eng A 503:156–159.
doi:10.1016/j.msea.2007.12.054

Nedjad SH, Teimouri J, Tahmasebifar A, Shirazi H, Ahmadabadi MN (2009b) A new concept in
further alloying of Fe-Ni-Mn maraging steels. Scr Mater 60:528–531. doi:10.1016/j.scripta
mat.2008.11.046

Nedjad SH, Meimandi S, Mahmoudi A, Abedi T, Yazdani S, Shirazi H, Ahmadabadi MN (2009c)
Effect of aging on the microstructure and tensile properties of Fe-Ni-Mn-Cr maraging alloys.
Mater Sci Eng A 501:182–187. doi:10.1016/j.msea.2008.09.062

Olson GB (1997) Computational design of hierarchically structured materials. Sci 277:1237–
1242. doi:10.1126/science.277.5330.1237

Pereloma EV, Shekhter A, Miller MK, Ringer SP (2004) Ageing behaviour of Fe-20Ni-1.8Mn-
1.6Ti-0.59Al (wt %) maraging steel: clustering, precipitation and hardening. Acta Mater
52:5589–5602. doi:10.1016/j.actamat.2004.08.018

Pereloma EV, Stohr RA, Miller MK, Ringer SP (2009) Observation of precipitation evolu-
tion in Fe-Ni-Mn-Ti-Al maraging steel by atom probe tomography. Metall Mater Trans A
40A:3069–3075. doi:10.1007/s11661-009-9993-z

Primig S, Leitner H (2010) Transformation from continuous-to-isothermal aging applied on a
maraging steel. Mater Sci Eng A 527:4399–4405. doi:10.1016/j.msea.2010.03.084

San Martin D, van Dijk NH, Jiménez-Melero E, Kampert E, Zeitler U, van der Zwaag S (2010)
Real-time martensitic transformation kinetics in maraging steel under high magnetic fields.
Mater Sci Eng A 527:5241–5245. doi:10.1016/j.msea.2010.04.085

Schnitzer R, Zickler GA, Zinner S, Leitner H (2009) Structure-properties relationship of a PH
13–8 Mo maraging steel. In: Beiss P, Broeckmann C, Franke S, Keysselitz B (eds) Tool
steels—deciding factor in worldwide production, Proceedings of the 8th International
Tooling Conference, vol I. Aachen, Germany, pp 491–503

Schnitzer R, Schober M, Zinner S, Leitner H (2010a) Effect of Cu on the evolution
of precipitation in an Fe-Cr-Ni-Al-Ti maraging steel. Acta Mater 58:3733–3741.
doi:10.1016/j.actamat.2010.03.010

Schnitzer R, Radis R, Nöhrer M, Schober M, Hochfellner R, Zinner S, Povoden-Karadeniz E,
Kozeschnik E, Leitner H (2010b) Reverted austenite in PH 13–8 Mo maraging steels. Mater
Chem Phys 122:138–145. doi:10.1016/j.matchemphys.2010.02.058

Schnitzer R, Zickler GA, Lach E, Clemens H, Zinner S, Lippmann T, Leitner H (2010c)
Influence of reverted austenite on static and dynamic mechanical properties of a PH 13–8 Mo
maraging steel. Mater Sci Eng A 527:2065–2070. doi:10.1016/j.msea.2009.11.046

Schnitzer R, Zinner S, Leitner H (2010d) Modeling of the yield strength of a stainless maraging
steel. Scr Mater 62:286–289. doi:10.1016/j.scriptamat.2009.11.020

Schober M, Schnitzer R, Leitner H (2009) Precipitation evolution in a Ti-free and Ti-containing
stainless maraging steel. Ultramicroscopy 109:553–562. doi:10.1016/j.ultramic.2008.10.016

Schober M, Lerchbacher C, Eidenberger E, Staron P, Clemens H, Leitner H (2010) Precipitation
behavior of intermetallic NiAl particles in Fe-6 at.%Al-4 at.%Ni analyzed by SANS and
3DAP. Intermetallics 18:1553–1559. doi:10.1016/j.intermet.2010.04.007

Sha W, Guo Z (2009) Maraging steels: Modelling of microstructure, properties and applications.
Woodhead Publishing, Cambridge. doi:10.1533/9781845696931

Shekhter A, Aaronson HI, Miller MK, Ringer SP, Pereloma EV (2004) Effect of aging and deformation on the microstructure and properties of Fe-Ni-Ti maraging steel. Metall Mater Trans A 35A:973–983. doi:10.1007/s11661-004-0024-9

Viswanathan UK, Dey GK, Sethumadhavan V (2005) Effects of austenite reversion during overageing on the mechanical properties of 18 Ni (350) maraging steel. Mater Sci Eng A 398:367–372. doi:10.1016/j.msea.2005.03.074

Wagner C (1961) Theory of the ageing of precipitates by redissolution (Ostwald maturing). Z Elektrochem 65:581–591

Xu W, del Castillo PEJRD, van der Zwaag S (2008) Computational design of UHS stainless steel strengthened by multi-species nanoparticles combining genetic algorithms and thermokinetics. In: New developments on metallurgy and applications of high strength steels, TMS, Warrendale, pp 1167–1181

Xu W, Rivera-Díaz-del-Castillo PEJ, van der Zwaag S (2009a) Computational design of UHS maraging stainless steels incorporating composition as well as austenitisation and ageing temperatures as optimisation parameters. Philos Mag 89:1647–1661. doi:10.1080/14786430903019081

Xu W, del Castillo PEJR, van der Zwaag S (2009b) A combined optimization of alloy composition and aging temperature in designing new UHS precipitation hardenable stainless steels. Comput Mater Sci 45:467–473. doi:10.1016/j.commatsci.2008.11.006

Xu W, del Castillo PRD, Yang K, Yan W, van der Zwaag S (2009c) Genetic computational design of novel ultra high strength stainless steels: model description and first experimental validation. In: TMS 2009 138th annual meeting and exhibition - supplemental proceedings, vol 2. Materials characterization, computation and modeling, TMS, Warrendale, pp 319–326

Xu W, Rivera-Díaz-del-Castillo PEJ, Yan W, Yang K, San Martín D, Kestens LAI, van der Zwaag S (2010a) A new ultrahigh-strength stainless steel strengthened by various coexisting nanoprecipitates. Acta Mater 58:4067–4075. doi:10.1016/j.actamat.2010.03.005

Xu W, Rivera-Díaz-del-Castillo PEJ, Wang W, Yang K, Bliznuk V, Kestens LAI, van der Zwaag S (2010b) Genetic design and characterization of novel ultra-high-strength stainless steels strengthened by Ni_3Ti intermetallic nanoprecipitates. Acta Mater 58:3582–3593. doi:10.1016/j.actamat.2010.02.028